Ion recognition properties of poly[Cu(3-MeOsalpd)] films

I. Kiersztyn · L. Neto · A. Carneiro · J. Tedim ·
C. Freire · A. R. Hillman

Abstract Poly[Cu(3-MeOsalpd)] films with good physical, chemical and electrochemical stability may be potentiodynamically electrodeposited with high deposition efficiency from acetonitrile solutions of the monomer. Comparative coulometric assays with the Ni-based analogue show that the metal in the *salen* motif does play a role in the electronic structure of the polymer, but that the electroactive response is ligand (not metal) based. The dynamics of redox switching are ultimately limited by coupled electron/counter ion diffusion, but this process is sufficiently rapid that it influences the voltammetric response only for thick films ($\Gamma > 420$ nmol cm^{-2}) at high scan rates. Redox cycling in monomer-free electrolyte shows a voltammetric signature that responds, *via* interaction with the pseudo-crown ether receptor sites, to the presence of Li$^+$, K$^+$, Mg^{2+} and Ba^{2+} ions in solution. The most prominent change is associated with the first anodic peak in the *i-E* signature. For each of the metal ions considered, this peak potential responds logarithmically to concentration in a manner that varies with individual complexed cation and film thickness and to an extent greater than predicted by the Nernst equation. The film characteristics offer some analytical promise, including a trade-off between sensitivity and dynamic range and signal amplification, possibly due to supramolecular effects.

Keywords Electroactive polymer · Thin film · *Salen* ·
Sensor · Ion recognition · Pseudo-crown ether

I. Kiersztyn · L. Neto · A. Carneiro · C. Freire (✉)
REQUIMTE/Departamento de Química e Bioquímica, Faculdade
de Ciências, Universidade do Porto,
Rua do Campo Alegre, s/n,
4169-007 Porto, Portugal
e-mail: acfreire@fc.up.pt

J. Tedim
CICECO, Departamento de Engenharia Cerâmica e do Vidro,
Universidade de Aveiro,
Campus Universitário de Santiago,
3810-193 Aveiro, Portugal

A. R. Hillman
Department of Chemistry, University of Leicester,
Leicester LE1 7RH, UK

Present Address:
A. Carneiro
Centre for Nanotechnology and Smart Materials,
4760-034 Vila
Nova de Famalição, Portugal

Introduction

Over the last few decades, the quest for novel materials based on electroactive polymers has motivated research in many areas, including electrocatalysis, [1], chemical sensors [1–5] and optoelectronics [1, 5, 6]. Among the vast range of molecular materials studied, promising systems include polymers based on metal complexes, in which the presence of the metal centres allows additional manipulation of electronic and chemical properties in comparison with organic-based polymers [7–13]. One of the categories of metal complexes that has attracted considerable attention is that based on the M(*salen*) motif [14, 15], for which the particular example studied here is shown in Scheme 1.

The attraction of the M(*salen*) motif lies in the ability separately to influence performance by variation of the metal (M) in the spine (Scheme 1, region I), by introduction of functionality in the imine bridge (region II) and by introduction (or not) of a second functionality in the aldehyde moiety (region III). In the present instance of a chemical sensor, the
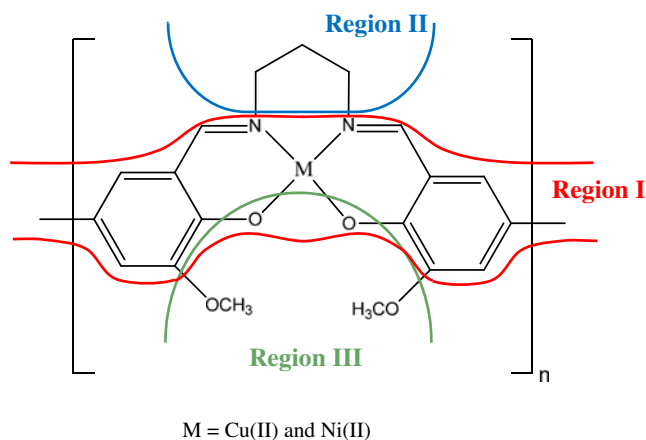
Scheme 1 Molecular structure of poly[Cu(3-MeOsalpd)] indicating the spinal *reporter*, imine bridge and pseudo-crown *receptor* components (regions I—III, respectively)

functionality is a *receptor*; more generally, other functionalities could be introduced for other applications. To anticipate some of the discussion below, when the motif is polymerized (as in Scheme 1), the *receptor* is to one side of the spine, which acts as a *reporter* via changes in the electrochemical response of the "molecular wire" resulting from extensive charge delocalisation in the polymer spine. The latter is analogous to the situation in a conducting polymer, such as polypyrrole or polythiophene, although the presence of the metal means that the underlying chemistry is somewhat different.

Recently, a number of studies involving electroactive polymer films have explored their application to ion recognition [3, 4, 16, 17]. The first example involving organic conducting polymers for ion recognition purposes was reported by Roncali et al. [17], who demonstrated that a polythiophene derivative showed specific interactions with Li^{+} cations. Since then, studies of polypyrrole [18–21] and polythiophene [22–26] films functionalized with ether-based (O donor) functionalities have been reported. An advantage of using polymeric (cf. molecular) electroactive sensing moieties is that even minor *molecular*-level interactions with the analyte may impart changes in collective properties at the *supramolecular* level, e.g. transport of species and/or conductivity [8]. This has the important effect of amplification of the recognition signal.

Viewed strategically, our early work on this class of materials focused on identification of the site of electroactivity [27–29]. FTIR and EPR spectroscopies, in conjunction with coulometry, showed this to be the ligand, not the metal [27, 30]; schematically this corresponds to region I of the monomer structure in Scheme 1. Subsequently, attention shifted to structural variation by substitution at the imine bridge (schematically, region II in Scheme 1). Based on established solution chemistry, we chose benzo crown ether substituents as metal ion receptors [31]. For complexes with methoxy substituents in the aldehyde moiety (see Scheme 1, region III), there is then

ambiguity regarding the receptor site: is it the benzo crown ether (in region II) or the pseudo crown (in region III)? Extended X-ray absorption fine structure (EXAFS) determination of the local environment around complexed barium ions showed that the crown ether was the receptor [31–33]. However, an important outcome is that in the spatially restricted film environment, the normal solution selectivity pattern (based on crown size) was lost [33]. Additionally, one might anticipate that sensitivity is diminished by the relatively large distance between the *receptor* and the *reporter*.

The generic aim of the present work is a means of identifying and quantifying ion binding for diverse alkali and alkaline earth ions; obvious variables are ion size and charge. Particular ions of interest are Li^{+} and Mg^{2+}. However, for these lighter (low Z) elements, our previous approach of using EXAFS to identify receptor location (which worked well for the high Z element Ba^{2+} [32, 33]) is not feasible. For this latter case, since the synthetic accomplishment of attaching a crown ether was not rewarded by control over selectivity based on crown size (see above), the strategy in the present work is to use the pseudo crown involving the methoxy groups. This shift in location of the *receptor* (from region II to region III in Scheme 1) places it closer to the *reporter* site (the polymer spine). An important question is whether this more intimate electronic coupling of *receptor* and *reporter* functionalities enhances sensing capability. One might hypothesise that the identity of the metal ion in the monomer complex may be more significant. Thus, although we focus on the Cu(*salen*) motif, we make comparison with the Ni analogue.

To summarise, the objectives are (1) quantitation of ion binding to a new *salen*-based polymer for group I and group II metal ions, (2) determination the effect (if any) of the imine bridge (e.g. through non-planarity effects on pseudo-crown geometry and spinal planarity) and (3) determination of the effect of the metal centre. The monomer from which the films are derived is [(bis(3-methoxysalicylidene)-2,3-propanodiiminato) M], henceforth abbreviated as [M(3-MeOsalpd)]. This work is distinct from our previous studies in three important respects: diversification from barium as target analyte, extension from a Ni- to a Cu-based complex and, in pursuit of possible sensing applications, quantitation of the electrochemical response to analyte concentration. The outcomes will be used to inform future DFT modelling of the complexes and their interactions with metal ions as a guide to synthetic effort.

Experimental

Materials

Acetonitrile (Romil, HPLC grade), tetrabuthylammonium perchlorate (TBAP, Fluka, puriss., electrochemical grade), tetraethylammonium perchlorate (TEAP, Fluka, puriss.,

electrochemical grade), LiClO$_4$, KClO$_4$, Mg(ClO$_4$)$_2$ and Ba(ClO$_4$)$_2$ (Aldrich +99.99%) were used as received. The monomers [M(3-MeOsalpd)] (M=Cu, Ni) were prepared by standard methods [34] and recrystallized from CH$_3$CN. Warning! Perchlorate salts are hazardous because of the possibility of explosion.

Instrumentation

Cyclic voltammetry was performed with an Autolab PGSTAT30 potentiostat/galvanostat. The electrochemical cell was a standard three-electrode cell. A Pt disk electrode with an area of 0.0314 cm^2 was used as working electrode and a Pt wire as a counter electrode. All potentials are referred to an Ag/AgCl (1 mol dm^{-3} NaCl) reference electrode. Prior to use, the Pt working electrode was polished with an aqueous suspension of 0.3 μm alumina (Beuhler) on a Master-Tex (Beuhler) polishing pad, then rinsed with water and ethanol, dried and finally rinsed with acetonitrile. All measurements were made at room temperature, T=20 (±2) °C.

Procedures

Poly[M(3-MeOsalpd)] films were deposited by immersing the electrode in a CH$_3$CN solution of 1 mmol dm^{-3} monomer/0.1 mol dm^{-3} R$_4$N$^+$ClO$_4^-$ (R=ethyl or butyl; see figure legends) at a scan rate, v=0.1 V s^{-1}. The potential range was −0.20 to 1.3 V for M=Ni and −0.40 to 1.40 V for M=Cu. Film thickness was varied via the number of potential cycles (see below for coulometric assay).

After electropolymerisation, the modified electrode was thoroughly rinsed with CH$_3$CN and transferred to 0.1 mol dm^{-3} R$_4$N$^+$ClO$_4^-$/CH$_3$CN solution. Film coverage and electroactivity were explored by potentiodynamic studies in the potential range −0.4 to 1.4 V at scan rates in the range 0.01 to 1.0 V s^{-1}. Interpretation of the coulometric data for polymerization and film deposition (via coupling of the

phenyl rings; see Scheme 1) (Q_{pol}) and for redox switching (Q_{redox}) is based on the established fact [27] that polymerization involves 2e per monomer unit. Reversible redox switching of the polymer is characterised by the transfer (in the parlance of electroactive polymers, "doping level") of y electrons per ring (i.e. $2y$ electrons per monomer unit) and z electrons per metal site. For simplicity, we will assign the symbol n to $2y$. The ratio of anodic charges passed in polymerization/deposition and subsequent voltammetry is $Q_{pol}/Q_{redox}=(2+n+z)/(n+z)$. Since z can only take the integer values 0 or 1 and n is positive, it turns out that the ratio Q_{pol}/Q_{redox} allows unique evaluation of n and z [27]. As discussed below, in the Ni case this procedure was restricted to very thin films due to deposition efficiency issues; no such restrictions arose for the Cu system of primary interest here.

Film responses to metal ions were determined by addition to background electrolyte of LiClO$_4$, KClO$_4$, Mg(ClO$_4$)$_2$ or Ba(ClO$_4$)$_2$; see figure legends for details. Evolution of i-E response was recorded after each addition until no further change occurred. At this point, the i-E response was determined as a function of scan rate.

Results and discussion

Film deposition

Figure 1 shows voltammetric responses acquired during representative [Ni(3-MeOsalpd)] and [Cu(3-MeOsalpd)] electropolymerization and deposition experiments, here using five polymerisation cycles. For [Ni(3-MeOsalpd)], the current starts to increase in the first half cycle at 0.65 V and two anodic waves at E_{paII}=0.71 V and E_{paIII}=0.96 V can be observed. On the reverse sweep three cathodic waves occur at E_{pcI}=0.14 V, E_{pcII}=0.36 V and E_{pcIII}=0.60 V. The second anodic half cycle shows a new broad anodic wave at E_{paI}=0.57 V, which is attributed to the oxidation of the previously
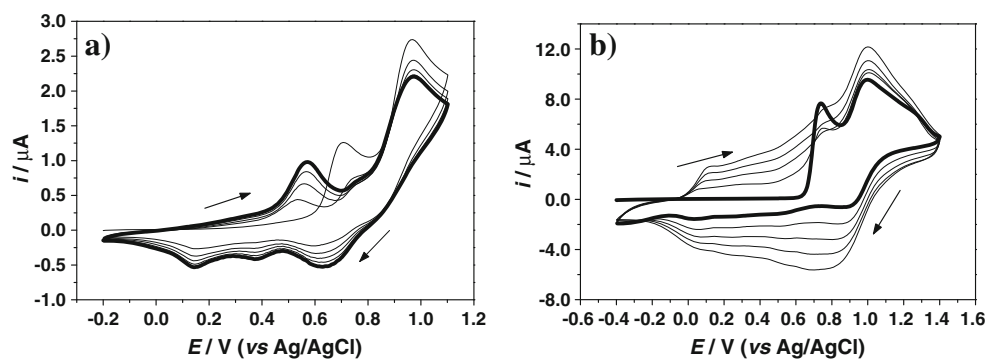

Fig. 1 Sequential cyclic voltammograms during potentiodynamic polymerisation at a Pt electrode of [Ni(3-MeOsalpd)] (a) and [Cu(3-MeOsalpd)] (b). In each case, the monomer concentration was 1 mmol dm^{-3}, the background electrolyte was 0.1 mol dm^{-3} TBAP/ CH$_3$CN and the scan rate, v=0.1 V s^{-1}. The total deposition process comprised five scans; the *bold line* in each case represents the response to the first scan

deposited film. In subsequent cycles, the features at E_{pI}, E_{pII} and E_{pIII} increase progressively in amplitude with the number of potential cycles.

In the case of [Cu(3-MeOsalpd)], the first half cycle of polymerisation shows a sharp increase in current at 0.68 V, two anodic waves at $E_{paII}=0.76$ V and $E_{paIII}=1.04$ V, and an incompletely resolved wave at $E_{paIV}=1.28$ V. On the reverse sweep, three cathodic waves occur at $E_{pcI}=-0.05$ V, $E_{pcII}=0.54$ V and $E_{pcIII}=0.92$ V, with E_{pcI} attributed to reduction of the previously deposited film. When the second cycle begins, a new anodic wave occurs at $E_{paI}=0.05$ V, which is attributed to the oxidation of film previously deposited during the first cycle. The current intensity associated with all these features increases as the number of deposition cycles increases.

Inspection of the working electrode surfaces at the end of the electrodeposition in both systems revealed the presence of insoluble films, yellow-greenish in colour for poly[Ni(3-MeOsalpd)] and green for poly[Cu(3-MeOsalpd)]. In the case of the Ni-based films, there was also visual observation of appreciable amounts of coloured particulates dispersed in solution; the relevance of this is discussed below in the context of coulometric assay of film deposition.

Film redox switching

In order to characterise the electrochemical properties of the deposited polymer films, the modified electrodes were immersed in monomer-free solution, to ensure that current features were attributable solely to the surface-bound structure. Figure 2 shows representative electrochemical responses for poly[Ni(3-MeOsalpd)] and poly[Cu(3-MeOsalpd)] films, namely those of Fig. 1.

Poly[Ni(3-MeOsalpd)] shows two anodic waves (at $E_{paI}=0.54$ V and $E_{paII}=0.82$ V) and three cathodic features (at $E_{pcI}=0.18$ V, $E_{pcII}=0.39$ V and $E_{paIII}=0.59$ V), whilst poly[Cu(3-MeOsalpd)] shows four anodic waves (at $E_{paI}=0.14$ V, $E_{paII}=0.64$ V, $E_{paIII}=0.91$ V and $E_{paIV}=1.09$ V), and four cathodic waves (at $E_{pcI}=0.09$ V, $E_{pcII}=0.35$ V, $E_{pcIII}=0.77$ V and $E_{pcIV}=1.12$ V). As is common for electroactive

polymer films, the i-E response during the first voltammetric cycle is anomalous (the so-called *first-cycle effect*). Assignment of the origin of this effect—most commonly to oxidation of residual monomeric/oligomeric species trapped into the polymeric matrix [35] or undefined "conditioning" of the film [36]—is outside the scope of this study; we focus on the properties of films once this process is complete.

Qualitative comparison between the voltammetric responses of poly[M(3-MeOsalpd)] films illustrates that poly[Cu(3-MeOsalpd)] shows a larger number of redox processes, spread across a wider potential range. Referring back to the objectives, this immediately signals that changing the metal centre from Ni to Cu influences film electrochemical response.

This change in electrochemical response requires confirmation (or otherwise) that, like poly[Ni(*salen*)]-type films, the Cu analogue electroactivity is ligand based. This may be inferred through coulometric determination of the oxidation degree, n (number of electrons per monomer unit involved in reversible film redox switching; see Experimental. For poly[Ni(3-MeOsalpd)], we find $z=0$ and $n=0.38$, and for poly[Cu(3-MeOsalpd)], we find $z=0$ and $n=0.21$. In both cases, the z values confirm the ligand-based nature of the redox processes. The n values correspond to delocalization of one charge over ca. three and five monomeric units, respectively. Inter-relation of these observations is beyond the scope of this experimental study, but will be the subject of a future DFT study.

The issue of attributing the current response of delocalised systems such as conjugated aromatic systems ("conducting polymers") into Faradaic and capacitive components has been the subject of longstanding debate [37]. The measurements made here do not contribute to this philosophical discussion. The practical distinction is that capacitive contributions will yield relatively flat (potential independent) responses, whereas the focus of our interest (see below) is the parameterization of current peaks (e.g. peak potentials). Hence, the presence or otherwise of capacitive effects will not influence the analytical utility of the film responses.

Coulometric estimates of surface coverage (Γ/mol cm^{-2}, where "mol" refers to moles of monomer units, determined

Fig. 2 Voltammetric responses of the films prepared in the experiment of Fig. 1, following transfer to monomer-free background. $\nu=0.1$ V s^{-1}. **a** Poly[Ni(3-MeOsalpd)]; **b** poly[Cu(3-MeOsalpd)]. *Asterisks* indicate features referred to in the main text
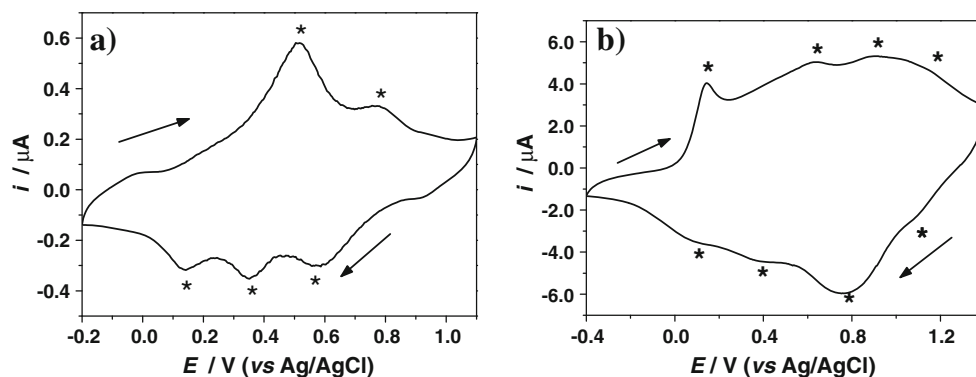
using the *n* values discussed above) are shown in Fig. 3 as a function of the number of deposition cycles for the two polymer types. For both films, Γ increases linearly until the ca. 50th deposition cycle, after which it increases less rapidly and ultimately reaches a limiting value after ca. 100 scans. The question of whether this represents a genuine limitation of coverage or is due to charge transport limitations is now addressed.

The Γ variations with number of deposition cycles (Fig. 3) imply that poly[Cu(3-MeOsalpd)] films grow ca. 100 times faster than poly[Ni(3-MeOsalpd)] films. Despite the similar polymerization charges (Q_{pol}) for the two complexes, the redox charges (Q_{redox}) were very different. As noted above, visual observation of extended poly[Ni(3-MeOsalpd)] deposition was accompanied by the generation of significant amounts of coloured material (oligomer and/or polymer) in the solution phase; this was not seen for the Cu case. This meant that the coulometric determination of *n*-values for poly[Ni(3-MeOsalpd)] was only possible for very thin films, for which no colouration of the solution in the vicinity of the electrode was observed; this was interpreted to signal minimal loss of material to solution. In practice, for the Ni-based films, we took the conservative approach of restricting use of this assay to film deposition by a single cycle. Thus, at least the majority of the difference in Γ values for the two systems (note the different coverage axis scales in Fig. 3) is attributable to film adherence—strong for the Cu polymer and weak for the Ni polymer.

Subsequent visual observation of the two film types, for similar numbers of deposition cycles, showed a much more optically dense deposit for the Cu system. Since the two monomers have broadly similar optical properties, this qualitatively supports the notion of low deposition efficiency for the Ni film, rather than charge transport limitations in its assay.
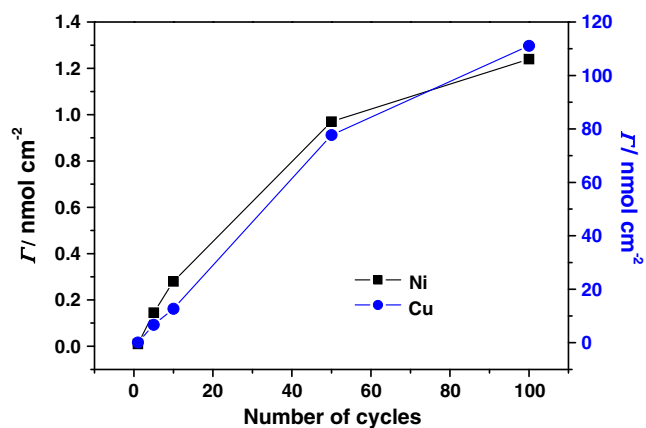

Fig. 3 Coulometrically estimated values of Γ (see main text for methodology and significance) as functions of the number of potentiodynamic polymerisation cycles for: *black square* (left hand axis) poly[Ni(3-MeOsalpd)] and *blue circle* (right hand axis) poly[Cu(3-MeOsalpd)]. *Lines* are merely a guide to the eye. Note the different scales for the two systems

For Cu films of high coverage, we postulate that the curvature in the plot of Γ vs. number of deposition cycles is attributable to charge transport limitations. This hypothesis is tested in the following section.

The end result of these preliminary experiments is that poly[Cu(3-MeOsalpd)] is the most promising system for ion recognition. We therefore focus on this system.

Film dynamics

The influence of experimental timescale on the voltammetric response of poly[Cu(3-MeOsalpd)] films was studied by potentiodynamic measurements in the range $0.01 < v/V \ s^{-1} < 1$. Figure 4 depicts representative data for poly[Cu(3-MeOsalpd)] films prepared with 5 and 50 polymerisation scans. The responses are representative of two classes of behaviour observed, according to film thickness, parameterized by Γ values (here, 66.5 and 510 nmol cm^{-2}, respectively). For thin films ($\Gamma < 420$ nmol cm^{-2}), both anodic and cathodic peak currents increased linearly with scan rate. Data for these and other examples within this class are summarised in Table 1, using the diagnostic parameter $d(\log i_p)/d(\log v)$: a value of 1 is the signature of a diffusionless system, commonly referred to as thin layer or surface-type behaviour [38]. In this case, irrespective of the underlying electron coupled ion motions, charge transport occurs on a shorter timescale than the experimental timescale. Other characteristics of this thin layer regime are symmetrically shaped redox waves and peak potentials independent of scan rate and scan direction ($E_{pa} \sim E_{pc}$), as seen in Fig. 4a.

For thick films ($\Gamma > 420$ nmol cm^{-2}), the situation is more complicated, since the diffusionless characteristics are seen at slow scan rates but not at high scan rates. Although the coalescence of individual peaks at high scan rate makes interpretation less easy, nonetheless it is clear that the evolution of voltammetric response with scan rate is different for thick films: at higher scan rates the cyclic voltammograms show tailing, typical of diffusionally controlled systems. Generally, when the diffusion of species is slower than the experimental timescale, the peak current changes linearly with $v^{1/2}$. This is identified through the diagnostic value of 0.5 for $d(\log i_p)/d(\log v)$ [39–41]. The transition towards this regime is clear in Fig. 4b, although the slopes collected in Table 1, with values of $d(\log i_p)/d(\log v) \sim 0.70$, do not attain the limiting value of 0.5 within the accessible range. The break point for the film of Fig. 4b ($\Gamma = 510$ nmol cm^{-2}) occurs at $v^* \sim 0.31$ V s^{-1} for the anodic process and $v^* \sim 0.24$ V s^{-1} for the cathodic process. These points also coincide with an increase in peak separation, $\Delta E_p > 0$.

The data of the previous paragraph allow some estimate of the diffusion coefficient (D/cm^2 s^{-1}) associated with charge transport in the film (thickness, h/cm) as follows. The characteristic timescale for diffusion in the film is $\tau_D = h^2/D$. The

Fig. 4 Timescale dependences of voltammetric responses of poly[Cu(3-MeOsalpd)] films to redox cycling in 0.1 mol dm^{-3} TBAP/CH$_3$CN. Panels **a** and **b** are for a film prepared by five deposition cycles (Γ=66.5 nmol cm^{-2}). Panels **c** and **d** are for a film prepared by 50 deposition cycles (Γ=510 nmol cm^{-2}). Panels **a** and **c** show raw data, namely *i-E* responses as a function of potential scan rate, 0.01<*v*/V s^{-1}<1.0 (as annotated). Panels **b** and **d** show plots of log (i_{paII}) and log (i_{pcIII}) vs. log ν. *Lines* represent least squares fits, with magnitudes of slopes, |*m*|
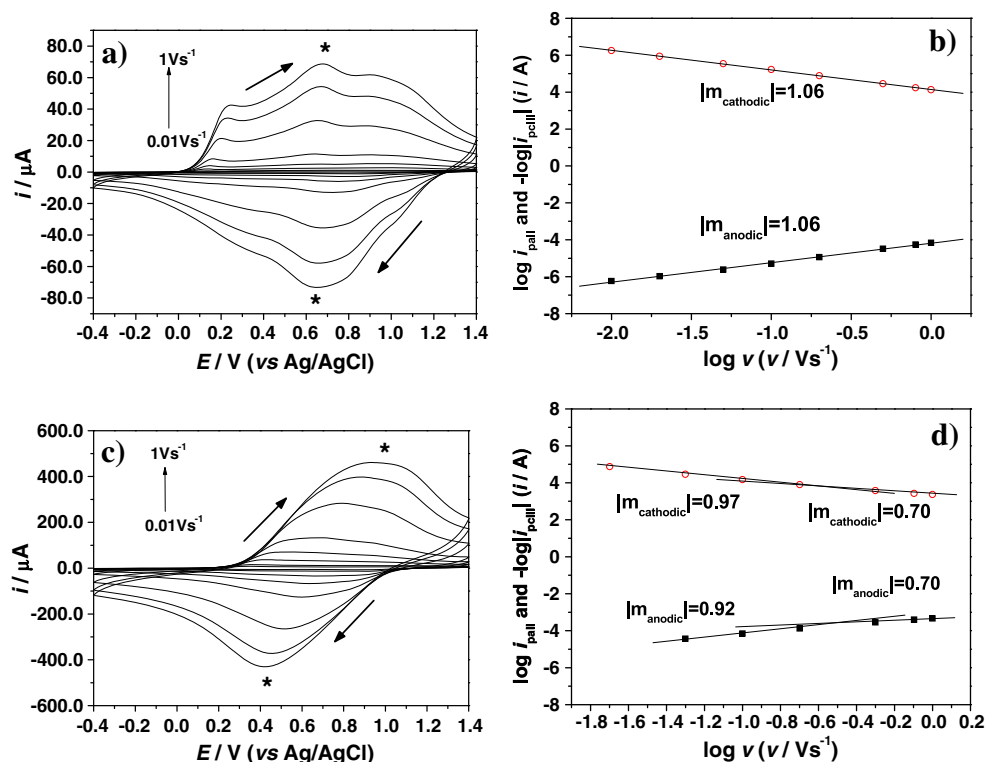
observational timescale of the experiment is $\tau_{CV}=RT/Fv*$. The break point occurs when $\tau_D=\tau_{CV}$. Inserting the value of $v*$ for the anodic process, we find $h^2/D=0.083$ s. Based on monomer molar mass, an assumption that the density of pure (unsolvated) polymer is the same as that of the monomer (1.4 g cm^{-3}) and a typical situation that a relatively soft film is swollen by a factor of 25–50% by solvent [29, 42, 43], we estimate the thickness of this particular film to be $h\sim1.5$ μm. On this basis, the effective diffusion coefficient for charge transport (representing coupled electron/ion motion) is $D\sim2\times10^{-9}$ cm^2 s^{-1}, which is typical for electroactive polymer films based on the M(*salen*)-motif and conducting polymers [27–29, 44]. At the level of precision

available, notably as limited by our knowledge of film swelling, the effective diffusion coefficients associated with polymer oxidation and reduction are essentially the same.

Identification of anion (here, perchlorate) as the transferred charge-balancing ion during redox switching in tetraalkylammonium salt solutions has been made gravimetrically for poly[M(*salen*)] films using the electrochemical quartz crystal microbalance (EQCM) [29, 31, 42, 43]. Solvent transfer also occurs, but the essential point in terms of electroneutrality is that anion transfer is dominant. XPS analysis of the Pd analogues [45] also shows that charge balance in the outer regions of such films is dominated by anion; it is unlikely that this dominance would be reversed in the film interior.

Table 1 Values of the slopes ($d\log i_p/d\log\nu$) for poly[Cu(3-MeOsalpd)] prepared with different number of polymerisation scans

No. of polymerisation scans	Γ (nmol cm^{-2})	Slopes ($d\log i_p/d\log\nu$)					
		Anodic[a]			Cathodic[a]		
		Low v	High v	Break point (V s^{-1})	Low v	High v	Break point (V s^{-1})
1	19.0	1.05	–	–	1.04	–	–
5	66.6	1.06	–	–	1.06	–	–
10	143	1.07	–	–	1.04	–	–
30	421	0.94	–	–	0.93	–	–
50	510	0.92	0.70	0.31	0.97	0.70	0.24

[a] Refers to annotated peaks in Fig. 4

Film response to metal cations

Exploitation of functionalised poly[M(*salen*)] to sense metal cations in solution involves *receptor* (pseudo crown) chemistry, *reporter* (ligand) redox chemistry and appropriate polymer/solution counter ion uptake (to maintain film electroneutrality).

Introduction of cationic species (here, Li^+, K^+, Mg^{2+}, Ba^{2+}) into solution then offers the possibility of partition into the film and binding to the pseudo-crown functionality (Scheme 1, region III). Our goal is to parameterize this process. The question then is the extent to which the presence of metal (in additional to tetraalkylammonium) cations may modify this situation.

Preliminary EQCM studies (Carneiro et al., unpublished work) show that there is redox-driven metal cation transfer when the solution concentration of these species is high. Although there is the obvious complication of the coordination chemistry, this is in many respects reminiscent of the phenomenon of permselectivity failure (exchange of co-ions as well as counter ions) that is well known in the ion-exchange literature [46]. From the perspective of ion sensing it is worth pointing out that ligand design focuses on moieties (here, pseudo-crown ethers) with high complexation constants, in order that the film can be used for low concentration analyses; in such situations, permselectivity failure will not occur. In other words, one can always impose permselectivity failure on the system by use of unrealistically high concentrations in a fundamental study, but it is not likely to be problematic in practice.

Figure 5 shows successive voltammetric responses of four nominally identical films (deposited by 5 cycles, final Γ=6.6–7.8 nmol cm^{-2}) to the addition of a given metal ion. The film responses evolve over a period of 10–15 redox cycles, more so for the anodic (cf. cathodic) features, dependent to some extent on the charge type of the cation. The common feature is the anodic shift of E_{paI}. In the case of alkali metals this shifts positively to 0.64 V, with an increase in peak current. For the alkaline earth cations, E_{paI} also moves towards more anodic potentials, but the corresponding peak current decreases. The most notable feature upon addition of Mg^{2+} or Ba^{2+} is the progressive increase of the peak current i_{paIII} for the anodic peak at E_{paIII}=1.09 V.

Turning to the cathodic features in the *i-E* curves, the peak currents at E_{pcI} and E_{pcIV} (i_{pcI} and i_{pcIV}, respectively) decrease upon addition of all the cations studied. The magnitude of i_{pcII} increases upon addition of alkali metal cations and decreases upon addition of alkaline earth metal cations, while that of i_{pcIII} increases upon K^+ and Ba^{2+} addition and decreases upon Li^+ and Mg^{2+} addition. Nevertheless, the changes in peak positions and amplitudes are much smaller than for their anodic counterparts.

To proceed further, it is necessary to select some specific feature(s) to quantify. As indicated above, the analyte-driven

changes in cathodic signature are too small to be of diagnostic or analytical value. Focusing on the anodic features, three candidate electrochemical parameters were chosen for more detailed evaluation of the ion recognition properties of poly[Cu(3-MeOsalpd)] films: E_{paI}, i_{paII} and i_{paIII}. The situation is summarised by Fig. 6, which collates the outcomes of the data in Fig. 5. (This collation of data for different films is made possible by the reproducibility of film deposition and response prior to metal ion addition; see Electronic supplementary material, Fig. S1.). Although i_{paII} and i_{paIII} do change with added metal cation identity and concentration (see above and Electronic supplementary material, Fig. S2), in practice, their value is largely limited to *qualitative* determination of the cation type. i_{paII} changes in the presence of alkali metal cations but not alkaline earth cations and vice versa for i_{paIII}. Beyond this, the relatively small changes and the challenge of estimating baseline currents reliably make quantitation difficult. In the light of the above, we focus primarily on changes in E_{paI}.

An encyclopaedic exploration of the variations of film response with film thickness, cation concentration and cation identity is beyond what can be shown here; a fuller exposition is given in the electronic supplementary material (see Figs. S2 and S3). Here, we explore in greater detail the most useful aspects. Figure 7 shows the variation of E_{paI} as a function of concentration of added cation for films prepared with ten deposition cycles ($\Gamma\sim1.0\times10^{-7}$ nmol cm^{-2}). As can be seen, this variation can be divided into two distinctive concentration regimes. The low concentration regime is characterised by a metal-dependent electrochemical response: the slopes $d(E_{paI})/d(\log$ [cation]) vary dramatically in the order $Li^+>Ba^{2+}\sim Mg^{2+}>K^+$. Interestingly, there is no obvious systematic variation with ion charge type. The high concentration regime has $d(E_{paI})/d(\log$ [cation]) slopes that are rather less diverse. This pattern of behaviour was observed for films prepared with one, five and ten deposition cycles ($18<\Gamma$/nmol cm$^{-2}<150$). We note that, for thicker films, the responses to Mg^{2+} and Ba^{2+} concentration are very similar.

The potentiodynamic experiments of Fig. 7 do not, by definition, yield potentiometric (equilibrium) measurements. Nonetheless, the most obvious way to consider variation of the intensive parameter E_p is as a function of log *c*, i.e. a pseudo-Nernstian response. In so doing, we make no thermodynamic assertion, but simply seek a practical way to consider the data. If the response were Nernstian and the films perfectly selective, then $d(E_{paI})/d(\log$ [cation]) would be 0.059 V/decade for the alkali and 0.029 V/decade for the alkaline earth cations [47], across the entire concentration range. We now explore the extent to which the films do (not) conform to this.

The full spectrum of responses, spanning variations of not only analyte concentration but polymer coverage (receptor population) and analyte type, is complex. Looking first at the
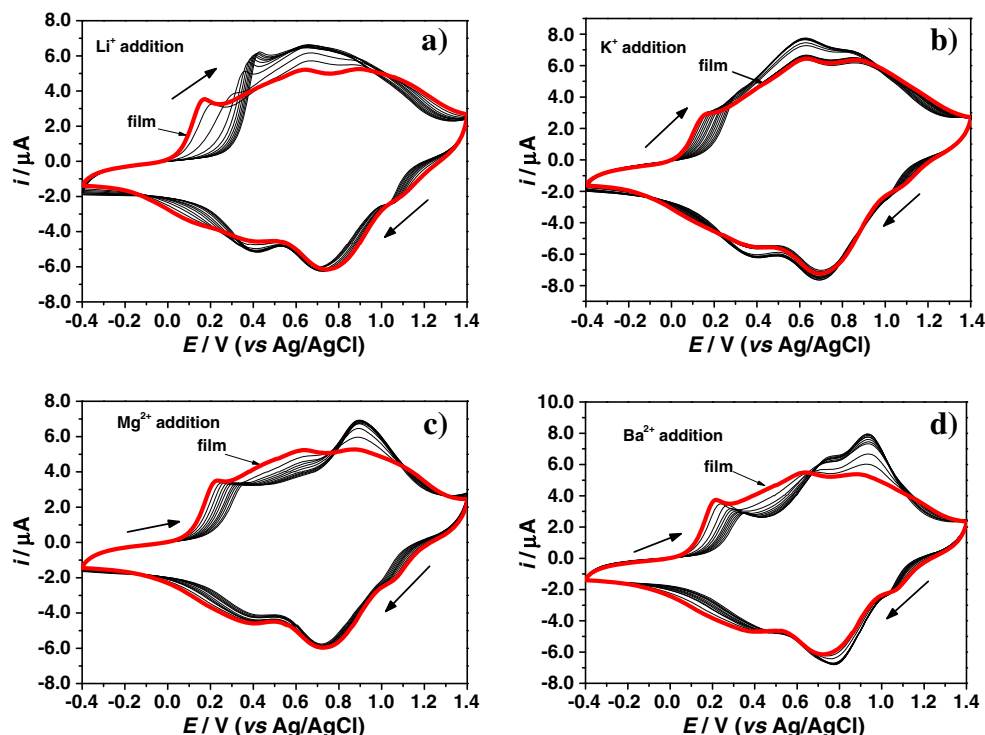
Fig. 5 Voltammetric responses of (ν=0.1 V s^{-1}) of poly[Cu(3-MeO-salpd)] films to the addition of metal ions: **a** Li$^+$; **b** K$^+$; **c** Mg^{2+}; **d** Ba^{2+}. Each *panel* is for a separate, but nominally identical, film prepared by five potentiodynamic deposition cycles (as in Fig. 4a). The initial response (*red trace*; marked "film") represents the response in metal ion-free background electrolyte (0.1 mol dm^{-3} TBAP/CH$_3$CN). Successive traces represent responses to sequential additions of 2 µl aliquots of 0.1 mol dm^{-3} solution (for Li$^+$, Mg^{2+} and Ba^{2+}) or 5 µl

aliquots of 2.5 mol dm^{-3} solution (for K$^+$), in each case as the perchlorate salt in CH$_3$CN. Based on simple arguments of added aliquot concentration and initial background electrolyte solution volumes, the final solution metal ion concentrations were: **a** [Li$^+$]=0.5 mmol dm^{-3}; **b** [K$^+$]=1.37 mmol dm^{-3}; **c** [Mg^{2+}]=0.5 mmol dm^{-3}; **d** [Ba^{2+}]= 0.5 mmol dm^{-3}. Typically, five cycles of evolution were taken for the steady state response to be established after each addition

variations with polymer coverage for a given anion (see Electronic supplementary material, Fig. S3), we find that the variation of E_{paI} with log c is simpler (closer to a single straight line) for thicker films. Although we have no direct structural

evidence, it would appear that the receptor sites are more heterogeneous in nature (variable binding energetics) in the thinner films and closer to homogeneous in the thicker films; the latter are more tractable to describe. Although there is no obvious fundamental reason for so doing (in the case of an
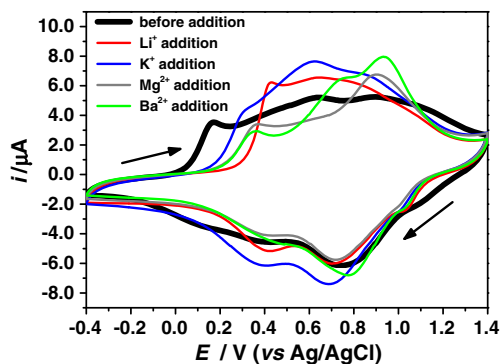

Fig. 6 Compilation of the final (high metal ion concentration) voltammetric responses of poly[Cu(3-MeOsalpd)] films deposited by five potentiodynamic cycles. Added metal ion (as the perchlorate salt) is: Li$^+$ (*red trace*); K$^+$ (*blue trace*); Mg^{2+} (*grey trace*); Ba^{2+} (*green trace*). The reproducible nature of the deposition process means that the "empty" receptor response ("before addition"; *black trace*) is essentially the same in all cases (see Electronic supplementary material, Figure S1). Data from Fig. 5
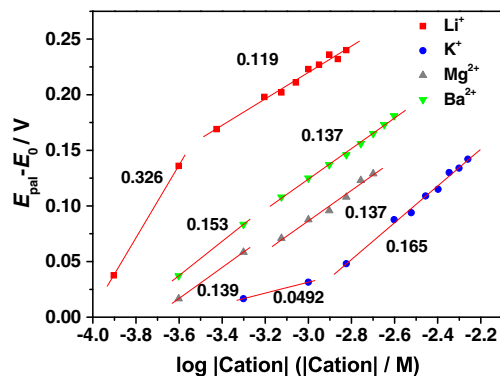

Fig. 7 Variation of E_{paI} (at steady-state response) as a function of added cation concentration (in logarithmic format) for poly[Cu(3-MeOsalpd)] films. Data acquired using experiments analogous to those in Figs. 5 and 6, except that the films were prepared using ten deposition cycles. Annotations adjacent to least squares fit *lines* indicate slopes (in V/decade)

intensive response parameter, E_p), we did consider attempting to normalise the response curves for films of different coverage (see Electronic supplementary material, Fig. S3) with respect to polymer coverage. However, even though such a manipulation does bring the curves closer together, there is no quantitative normalisation.

One interesting observation relates to a trade-off between sensitivity and dynamic range, as follows. For any given analyte cation, the range of observed E_{paI} values (running from the value for the empty receptors to saturation) is broadly the same. For thin films, the potential responds more sharply to analyte concentration, i.e. shifts across the dynamic range over a relatively narrow range of concentration ($c \leq 0.5$ mmol dm^{-3}), while for thick films the same response range is traversed over a concentration range around an order of magnitude larger.

Focusing on the thick film data (Fig. 7), the *Nernst-like* slopes at low concentration vary by a factor of ca. 6 (Li$^+$, 0.326 V/decade; K$^+$, 0.049 V/decade; Mg^{2+}, 0.139 V/decade; Ba^{2+}, 0.153 V/decade) and their relative values do not follow the variation of cation charge. (We consider only the slopes, i.e. relative changes in response; as is common, practical application would involve a calibration to place these responses on an absolute concentration scale.). Additionally, with the possible exception of K$^+$, the absolute values are not in accord with any simple prediction. At high concentration, there is greater uniformity of behaviour, although there is still no conformity to the Nernst equation. Interestingly, the greater slopes (by a factor of ca. 2 for the alkali metals and ca. 4 for the alkaline earth metals) imply greater sensitivity.

To rationalise the observed behaviour, we note that the present situation can be likened to one category of *three phase electrode* [48], in which the three phases are the substrate electrode (phase I), the polymer film (phase II) and the electrolyte solution (phase III), where the nomenclature follows that used by Scholz et al. [48]. In the physical case considered here, phase II is redox active, so there can be electron transfer between phases I and II and ion exchange between phases II and III. These electron and ion-exchange equilibria are coupled by the electroneutrality constraint. At equilibrium, one can write logarithmic (Nernstian-like) expressions linking the potential and the activities of the species. This may be done for the individual processes, i.e.:

$$E_{I/II} = E^0_{Ox/Red} + \frac{RT}{nF} \ln\left\{ \frac{\alpha_{Ox}}{\alpha_{Red}} \right\} \quad (1)$$

for an n-electron Ox/Red redox couple in phase II and

$$E_{II/III} = E^0_C + \frac{RT}{nF} \ln\left\{ \frac{\alpha_{C_{III}}}{\alpha_{C_{II}}} \right\} \quad (2)$$

for the exchange of the counter ion C between phases II and III, where in each instance a represents the activity of the subscripted species. These expressions may be unified in a single, more complex expression:

$$E = E^0_{Ox/Red/C} + \frac{RT}{nF} \ln\left\{ \frac{\alpha_{Ox}\, \alpha^n_{C_{III}}}{\alpha_{Red}\, \alpha^n_{C_{II}}} \right\} \quad (3)$$

This predicts the classical $59/n$ mV per decade slope for E vs log a plots. It is clear from the data in Figs. 5, 6 and 7 that there is not a simple—or indeed even a single (for a given charge type)—relationship of this form between the peak potentials and the concentrations of the exchanged metal ions. One may postulate a number of reasons for the observed deviations from the simple behaviour represented by the above expressions. We consider five physically plausible possibilities: two kinetic, two thermodynamic and one supramolecular in nature.

The first consideration is the rather obvious point that a potentiodynamic experiment is, by definition, not associated with a static boundary condition. The complexities of kinetic effects are well appreciated [48]. Notwithstanding this, it is a common practice to interpret data from voltammetric experiments according to these equilibrium expressions. The criterion for doing so is that the timescale of the experiment is sufficiently long that kinetic (and transport) phenomena do not dominate the response. In the present context, this is addressed by using sufficiently potential slow scan rates that the peak potential does not vary with scan rate. Data of the type shown in Fig. 4 (and analogues) show that this can be accomplished using a suitable combination of (low) film thickness and (slow) scan rate. We therefore reject this possibility.

The second possibility invokes what has been referred to as *phase-like behaviour* [49], in which there is a very different relationship between redox site population (as determined by film charge) and its activity. In one scan direction, the film consists of a spatially homogeneous mixture of Ox and Red sites (with the corresponding counter ion populations), such that the activities of both species vary continuously (though not necessarily linearly; see below) with film charge. In the other scan direction, there is a region of pure Ox or Red, which grows or shrinks (according to the species involved) with injected charge. The activity of this region (as a pure phase) is unity, creating the unusual situation that the amount (population) varies with charge but the activity is constant until a dramatic change upon complete consumption of the species at the end of the process. This situation was described for polyvinylferrocene films in selected solvents [49] and was identified by characteristic i-E signatures, of a form we do not see here. We therefore reject this possibility.

The third possibility is associated with the difficulty of quantifying the Gibbs energy of ion transfer between phases

II and III (in the nomenclature of ref. 41). One might consider attempting to gain insight via separate measurements of the Gibbs energy of transfer between water and an organic solvent. The difficulty here is that plausible organic solvents for such a measurement are unlikely to mimic the characteristics of the redox active polymer: the former are small saturated molecules carrying no charge, while the latter comprises large molecules with extended conjugation and relatively high (and variable) charge density. Although this source might well contribute to the response, there is no direct evidence for it doing so. Furthermore, pursuit of this speculation would require an experimental and theoretical study that is beyond the scope of the present work.

The fourth candidate explanation is based on the fact that the Nernstian-type expressions above involve the *activities* of the various species involved but, aside from the ions in the solution (phase III) these are not accessible quantities. Rather, probes of these other species yield populations (or changes therein) that relate directly to *concentrations*. For example, coulometric assays of redox species (using Faraday's law) yield populations of electroactive species and gravimetric assays (using acoustic wave devices such as the QCM) yield population changes of transferred species. Relating these to activities requires knowledge of the relevant activity coefficients. That the activity coefficients of both fixed sites and the species that permeate them (ions and solvent) deviate significantly from unity in media of the type represented by an electroactive film is well appreciated in an extensive classical ion-exchange literature [46] and has been considered in the context of electroactive films [50]. Consequently, there is no question that this will be a major contributor to the potential responses generated by ion uptake of the films. The practical limitation is that, while some trends might be rationalised *a posteriori* at a qualitative level, there is no generally applicable model for a *priori* calculation of activity coefficients in media of this type.

The final possibility is a more overtly chemical feature of the interaction of the metal ion with the *reporter* moiety. The postulate is that the delocalized nature of the electroactive probe results in a supramolecular effect that acts as a chemical amplification.

In conclusion, under the conditions employed, we reject kinetic factors as significant contributors to the supra-Nernstian slopes, recognise that partition energetics may be a modest factor and deduce that non-ideality effects (activity coefficient variations) are likely to be a major factor in this respect. We also postulate that supramolecular effects might be significant.

This last possibility raises the question of the nature of the interaction of the coordination metal ion with the polymer and its influence on redox activity of the polymer via its electronic structure. Interrogation of the latter is best addressed spectroelectrochemically. We have shown for poly[Cu(*salen*)] and poly[Pd(*salen*)] films [45, 51] that even Cu or Pd vs Ni replacement *within* the delocalized system does not change the ligand-based spectroelectrochemical response; in some respects this is surprising, but it is the observed result. Aside from minor changes in coordination bond lengths, EXAFS data [32, 33, 45] show that poly[M(*salen*)] film structures are generally insensitive to metal ion coordination, both within the polymer spine and, even for ions as large as Ba^{2+}, within the pseudo-crown functionality [32, 33]. This body of evidence suggests that metal ion coordination within the pendant crown ether functionality is unlikely to exert a large perturbation on the spinal electronic structure and thence electrochemical response. The question of the influence of crown-complexed metal ions on film redox response is more subtle. Although the above observations show that the basic polymer structure is retained, complexation may modulate the electron distribution within this framework: any such changes are manifested via changes in voltammetric peak potentials. These will be more significant when the complexation site is the pseudo-crown pocket (region III in Scheme 1), due to the proximity of the metal cation to the redox "reporter" functionality (region I in Scheme 1). In systems where the complexation site is a pendant crown ether functionality in region II [33], tethered at some distance from the "reporter" by a saturated alkyl linkage, the effect will be small. To conclude, although there is no change in the ligand-based oxidation mechanism, the presence of complexed metal cation sufficiently close to the polymer spine may significantly influence the electron density there and thence shifts the E_p. Although we do not attempt to quantify such effects, the presence of the metal cation might be expected to make removal of electrons from the film more difficult, i.e. to cause a positive shift in redox potential: commonly this is observed.

In Fig. 4 and Table 1, we considered the dynamics of film redox switching in the absence of added metal cation. We now consider the analogous data following the addition of metal cation, with the goal of determining whether the uptake of metal ions by the receptor inhibits ligand-based electron transport or (more likely) coupled counter ion transport. The results of potentiodynamic studies acquired for films after cation uptake are summarised in Table 2. The log i_p vs log v plot slopes are, within experimental uncertainty, unity, i.e. typical of a thin layer (surface-type) regime for charge transport. Therefore, although the presence of the small cations induces modifications in the electrochemical response of the modified electrodes, they do not observably inhibit coupled electron/counter ion transport. Expressed slightly differently, uptake of the solution cations modifies the *shape* of the i-E curve—indeed, this is the basis of their detection—but not its *area*, i.e. not the total charge encompassed by it.

The one exception to this behaviour was obtained for a film prepared with one deposition cycle upon Mg^{2+} addition,

Table 2 Values of the slopes ($d\log i_p/d\log\nu$) for poly[Cu(3-MeOsalpd)] prepared with different number of polymerisation scans, after cation additions

Cation	No. of polymerisation scans	Γ (nmol cm^{-2})	Slopes ($d\log i_p/d\log\nu$) Anodic[a]			Cathodic[a]		
			Low ν	High ν	Break point (V s^{-1})	Low ν	High ν	Break point (V s^{-1})
Li$^+$	1	18.3	1.01	–	–	1.02	–	–
	5	78.5	1.13	–	–	1.02	–	–
	10	146	0.90	–	–	0.99	–	–
K$^+$	1	20.9	0.99	–	–	1.02	–	–
	5	65.8	0.92	–	–	0.96	–	–
	10	146	0.87	–	–	0.92	–	–
Mg^{2+}	1	23.5	0.83	0.76	0.037	0.93	–	–
	5	67.0	1.07	–	–	0.95	–	–
	10	130	1.08	–	–	0.95	–	–
Ba^{2+}	1	20.3	0.96	–	–	0.99	–	–
	5	71.1	1.06	–	–	0.97	–	–
	10	145	0.89	–	–	0.91	–	–

[a] Refers to most intense peaks in Fig. 5

where the beginnings of transport limitation were observed. We have no clear explanation for this anomaly, although it may be due to loss of electroactivity in the outer region of the film, inhibiting interfacial ion transfer.

Conclusions

Poly[Cu(3-MeOsalpd)] films with good physical and (electro)chemical stability and of controllable coverage may be potentiodynamically electrodeposited from acetonitrile solution of the monomer. Subsequent film redox cycling in monomer-free electrolyte shows a complex, but reproducible, voltammetric signature. Coulometric assays of the deposition and redox cycling processes show that film electroactivity is ligand based and that the highest oxidation state corresponds to one positive charge delocalized over ca. 5 monomer units.

Redox switching of relatively thin poly[Cu(3-MeOsalpd)] films ($\Gamma < 420$ nmol cm^{-2}) is complete on the timescale of typical voltammetric experiments. For thicker films ($\Gamma > 420$ nmol cm^{-2}, typically deposited by >50 potentiodynamic cycles), diffusionless characteristics are seen only at low potential scan rates. At high scan rates, the peaks broaden, show diffusional tailing and start to coalescence. The transition between these two regimes can be used to estimate a coupled electron/ion diffusion coefficient, $D \sim 2 \times 10^{-9}$ cm^2 s^{-1}.

Voltammetric signatures of poly[Cu(3-MeOsalpd)] films respond to addition of Li$^+$, K$^+$, Mg^{2+} and Ba^{2+} and evolve over 10–15 redox cycles. The common feature is an anodic shift of the first anodic peak, parameterized via the peak

potential (E_{paI}). The cathodic features in the i-E curves show much smaller changes in position and amplitude with added metal cation; they are not diagnostically or analytically useful.

Although potentiodynamic experiments are not (by definition) equilibrium measurements, it turns out to be useful to consider the variations in peak potential in a pseudo-Nernstian manner, i.e. via E_{paI} vs. log c plots. Such plots can be divided into two distinctive concentration regimes. The low concentration regime is characterised by a highly metal-dependent electrochemical response, with slopes decreasing in the order Li$^+$ > Ba$^{2+} \sim$ Mg^{2+} > K$^+$. The high concentration regime has d(E_{paI})/d (log c) slopes that vary rather less. The variation of E_{paI} with log c is simpler for thicker films; this suggests that the receptor environments in thicker films are more homogeneous.

There is an interesting trade-off between sensitivity and dynamic range. For addition of a given analyte cation, the span of E_{paI} values is broadly the same, but for thin films the potential responds more sharply to analyte concentration (higher sensitivity, but narrower dynamic range); the reverse is true for thick films. For thick films, the E_{paI} vs log c slopes are generally much greater than a Nernstian-type response. We suggest that this may be a supramolecular effect, based on the interaction of the *receptor* with the *reporter* spine. Irrespective of its origin, this has the practical value of signal amplification. Exploration and optimization of these parameters is the natural future development of the present fundamental study.

References

1. Lua X, Zhanga W, Wanga C, Wenb TC, Weic Y (2011) Prog Polym Sci 36:671–712
2. Hua D, Xiaodong C, Ming LC (2009) ACS Appl Mater Interfaces 1:1599–1606
3. McQuade T, Pullen AE, Swager TM (2000) Chem Rev 100:2537–2574
4. Kazunori S, Swager TM (2007) B Chem Soc Jpn 80:2074–2083
5. Francisco RR, David Z, Carlos A (2010) Polymer 51:308–315
6. Moliton A, Hiorns RC (2004) Polym Int 53:1397–1412
7. Schaferling M, Bauerle P (2001) Synthetic Met 119:289–290
8. Sylvie CN, Aymeric P, Garth C, Deronzier A (2006) J Electroanal Chem 597:28–38
9. Byrne PD, Mueller P, Swager TM (2006) Langmuir 22:10596–10604
10. Junhua Y, Dongxue H, Yuanjian Z, Shen YF, Wang Z, Zhang Q, Niu L (2007) J Electroanal Chem 599:127–135
11. Schmittel M, Lin H (2008) J Mat Chem 18:333–343
12. Fabre B, Hao E, LeJeune ZM (2010) ACS ACS Appl Mater Interfaces 2:691–702
13. Joseph A, Ramamurthy PC, Subramanian S (2012) J Appl Polym Sci. doi:10.1002/app.34561
14. Whiteoak CJ, Salassaa G, Kleij AW (2011) Chem Soc Rev. doi:10.1039/c1cs15170c
15. Kleij AW (2008) Chem Eur J 14:10520–10529
16. Swager TM (1998) Acc Chem Res 31:201–207
17. Roncali J, Garreau R, Delabouglise D, Garnier F, Lemaire M (1989) J Chem Soc Chem Commun 679–681
18. a) Youssoufi HK, Hmyene M, Garnier F, Delabouglise D (1993) J Chem Soc Chem Commun 1550–1552
19. Garnier F, Korri H, Hmyene M, Yassar A (1994) Polym Prep 35:205–208
20. Youssoufi HK, Yassar A, Baiteche S, Hmyene M, Garnier F (1994) Synth Met 67:251–254
21. Ion A, Ion I, Popescu A, Ungureanu M, Moutet JP, Saint-Aman E (1997) Adv Mater 9:711–713
22. Baüerle P, Scheib S (1993) Adv Mater 5:848–853
23. Marsella MJ, Swager TM (1993) J Am Chem Soc 115:12214–12215
24. Swager TM, Marsella MJ (1994) Adv Mater 6:595–597
25. Baüerle P, Scheib S (1995) Acta Polym 46:124–129
26. Reddinger JL, Reynolds JR (1998) Chem Mater 10:3–5
27. Vilas-Boas M, Freire C, de Castro B, Christensen PA, Hillman AR (1997) Inorg Chem 36:4919–4929
28. Vilas-Boas M, Freire C, de Castro B, Hillman AR (1998) J Phys Chem B 102:8533–8540
29. Vilas-Boas M, Santos IC, Henderson MJ, Freire C, Hillman AR, Vieil E (2003) Langmuir 19:7460–7468
30. Vilas-Boas M, Freire C, de Castro B, Christensen PA, Hillman AR (2001) Chem Eur J 7:139–150
31. Martins M, Freire C, Hillman AR (2003) Chem Commun 434–435
32. Tedim J, Carneiro A, Bessada R, Patrício S, Magalhãs AL, Freire C, Gurman SJ, Hillman AR (2007) J Electroanal Chem 610:46–56
33. Tedim J, Bessada R, Patrício S, Magalhães AL, Freire C, Gurman SJ, Hillman AR (2008) Langmuir 24:8998–9005
34. Freire C, de Castro B (1998) Polyhedron 17:4227–4235
35. Goldsby KA (1988) J Coord Chem 19:83–90
36. Dahm CE, Peters DG, Simonet J (1996) J Electroanal Chem 410:163–171
37. Feldberg S (1984) J Am Chem Soc 104:4671–4674
38. Kelly DM, Vos JG (1994) In: Lyons MEG (ed) Electroactive polymer electrochemistry. Part 1. Fundamentals, Chap. 8. Plenum Press, New York
39. Bedioui F, Voisin M, Devynck J, Bied-Charreton C (1991) J Electroanal Chem 297:257–269
40. Martin CR, Rubinstein I, Bard AJ (1982) J Am Chem Soc 104:4817–4824
41. Bartlett PN (1987) In: Turner APF, Karube I, Wilson GS (eds) Biosensors: fundamentals and applications, Chap. 13. Oxford University Press, Oxford
42. Vilas-Boas M, Henderson MJ, Freire C, Hillman AR, Vieil E (2000) Chem Eur J 6:1160–1167
43. Tedim J, Freire C, Hillman AR (2009) Soft Matter 5:2603–2613
44. Oyama N, Ohsaka T (1992) In: Murray RW (ed) Molecular design of electrode surface, Chap. VIII. Wiley, New York
45. Fonseca J, Tedim J, Biernacki K, Magalhães AL, Gurman SJ, Freire C, Hillman AR (2010) Electrochim Acta 55:7726–7736
46. Marinsky JA (1976) Coord Chem Rev 19:125–171
47. Bard AJ, Faulkner LR (2001) Electrochemical methods, fundamentals and applications, 2nd edn. Wiley, New York
48. Scholz F, Schroder U, Gulabowski R (2005) Electrodes with immobilizaed particles and doplets—three-phase electrodes. In: Electrochemistry of immobilized particles and droplets, chapter 2. Springer, Berlin, pp 11–18
49. Daum P, Murray RW (1981) J Phys Chem 85:389–396
50. Bruckenstein S, Hillman AR (1988) J Phys Chem 92:4837–4839
51. Martins M, Vilas-Boas M, Freire C, Castro B, Hillman AR (2005) Electrochim Acta 51:304–314